Journal of King Saud University – Science 35 (2023) 102921

HOSTED BY

Contents lists available at ScienceDirect

Journal of King Saud University – Science

journal homepage: www.sciencedirect.com

Original article

Enhanced corrosion inhibition effect of sodium tartrate on copper in potable water

Ramasamy Sudhakaran [a,*], Thiagarajan Deepa [b], Munusamy Thirumavalavan [c,*], Sharmila Queenthy Sabarimuthu [c], Sellamuthu Babu [a], Thayuman Asokan [a], Abdulrahman I. Almansour [d], Pandian Bothi Raja [e], Karthikeyan Perumal [f]

[a] PG & Research Department of Chemistry, Government Arts College, Tiruchirappalli 620 022, Tamil Nadu, India, Affiliated to Bharathidasan University, Tiruchirappalli 620 024, Tamil Nadu, India
[b] PG & Research Department of Chemistry, Government Arts College, (Autonomous), Karur 639 005, Tamil Nadu, India, Affiliated to Bharathidasan University, Tiruchirappalli 620 024, Tamil Nadu, India
[c] Department of Chemistry, Saveetha Engineering College, Saveetha Nagar, Thandalam, Chennai 602105, Tamil Nadu, India
[d] Department of Chemistry, College of Science, King Saud University, P.O. Box 2455, Riyadh 11451, Saudi Arabia
[e] School of Chemical Sciences, Universiti Sains Malaysia, 11800 Penang, Malaysia
[f] Department of Chemistry and Biochemistry, The Ohio State University, 151 W. Woodruff Ave, Columbus, OH 43210, USA

ARTICLE INFO

Article history:
Received 27 May 2023
Revised 21 July 2023
Accepted 26 September 2023
Available online 4 October 2023

Keywords:
Corrosion
Copper
Electrochemical studies
SEM
EDAX
AFM
Water contact angle

ABSTRACT

In this study we have reported sodium tartrate (ST) and Zn^{2+} as the potential mixed corrosion inhibitors for copper corrosion in drinking water, by using electrochemical impedance and polarization techniques. The results of potentio-dynamic polarization indicated that sodium tartrate could be used as mixed type inhibitor with Zn^{2+}. ST was found to be 92% effective for slowing down both the anodic and cathodic reaction rates. It was additionally found that ST could coat the surface of copper to prevent it from conducting electricity. As the inhibitor concentration increased, the stability of the formed protective layer was also improved. The results obtained from studies like SEM, EDAX, AFM, and water contact angle clearly indicated the development of a barrier by inducing the lotus effect on copper surface. The water contact angle measurement results suggested that the coating formed in the presence of inhibitor was superhydrophobic, and the surface was homogeneous.

1. Introduction

A 3–4% loss of world's GDP productivity is mainly due to corrosion in industry. However, another 20% of this loss can be prevented by the use of proper corrosion protection methods (Philip and Schweitzer, 2010; Finšgar and Milošev, 2010). Thus, the goal of corrosion study has been to find ways to diminish or prevent the damage. Copper due to its good properties has wide range of applications. However, despite its significant resistivity, it would be susceptible to corrosion in aggressive conditions (Antonijević and Petrovic, 2008). Thus, it is necessary to use the corrosion inhibitors in such conditions to prevent the copper corrosion. The dissolution of copper at anodic site is the main reason for the corrosion process. The electrode reactions on the copper surface can generally control copper dissolution and corrosion rates (Kear et al., 2004). Corrosion inhibitors are used to reduce copper rust because they can slow down corrosion when the metal is exposed to harsh conditions or when corrosive ions like chloride or sulphate are present. Studies reported that both anodic and cathodic corrosion could be reduced by using corrosion inhibitors (Cao, 1996). The anodic dissolution of copper is decelerated, and at the cathode the amount of oxygen or hydrogen reduced on the surface of copper when an inhibitor is added to a corrosive environment. The concurrent inhibition of the anodic and cathodic corrosion can be achieved with the help of a mixed inhibitor (Khaled and Hackerman, 2003).

* Corresponding authors.
E-mail addresses: drrskchem@gmail.com (R. Sudhakaran), mtvala@gmail.com (M. Thirumavalavan).
Peer review under responsibility of King Saud University.

Production and hosting by Elsevier

https://doi.org/10.1016/j.jksus.2023.102921
1018-3647/

Mostly nitrogen/sulphur/phosphorous-containing heterocycles can act as inhibitors to protect the metal surfaces from deterioration in acidic environments (Habib, 1998; Mohanasundaram et al., 2022; Feng et al., 2011) due to the coordination behavior of these heterocycles with the metal atoms (Antonijević and Petrovic, 2008). The efficiency in inhibiting the corrosion is an important factor to consider when determining how effective a corrosion inhibitor would be in a given setting (which is estimated from variations in corrosion rate). It is well recognized that a number of variables, including the kind of metal, the environment, the chemical make-up and structure of the corrosion inhibitor, and the electrical (electrostatic) characteristics of the corrosion inhibitor, can affect its effectiveness. It is noteworthy to mention that the effectiveness of corrosion inhibitors has increased and thanks to the research and development. The studies indicated that the capability of corrosion inhibitors to prevent copper from corrosion could be determined by their ability to form a film via polymerization, p-p and vander waals contacts, bond strength to the surface of metal, and the presence of heteroatoms such as oxygen, nitrogen, and Sulphur. It was suggested that the stability in extreme conditions, including temperature, pH, and the presence of corrosive elements, would be particularly crucial (Ramesh and Rajeswari, 2005; Szőcs et al., 2005). Generally, ions of organic acids with nucleophilic substituents (Cabrin et al., 2020) show the ability to act as corrosion inhibitors due to their coordination ability to the metal surface. Thus, tartrate-based inhibitors are thought to be the most effective and thanks to their chelating ability, (Cabrin et al., 2020).

The primary goal of the current study was to use electrochemical methods to investigate the anti-corrosion effects of sodium tartrate and Zn^{2+} on copper in potable water. In this study, the surface coating was examined by utilizing the surface analytical techniques.

2. Materials and methods

2.1. Materials

A copper steel with composition of 1.57% Zn, 0.0053% Si, 0.0297% Fe, 0.0103% Ni, and 0.0087% Cu was used for corrosion prevention studies. Press cuts, machining, and emery papering were used to create copper specimens that measured 1.0 × 4.0 × 0.2 cm. Then, it was rinsed with acetone and double distilled water before being air-dried. Prior to any experiment, substrates were made as stated above and used immediately. Both Zn^{2+} and ST were incorporated as such without any changes. A 1000 ppm stock solution was used to further prepare the various diluted solutions (concentrations) of ST. In this work. drinking water from Perambalur, Tamil Nadu, India was utilized for all of the solutions. This research work was conducted at normal room temperature. Table 1 displays its physicochemical parameters of potable water.

Table 1
List of Physico-chemical parameters of potable water.

Parameters	Values
pH	7.84
Total Hardness	102 ppm
TDS	251 ppm
Conductivity	358 µmhos/cm
Alkalinity	113 ppm
Chloride	30 ppm

2.2. Electrochemical studies

An electrochemical workstation (model CHI-60D) was used in order to carry out the conducting electrochemical impedance spectroscopic (EIS) studies and potentio-dynamic polarization studies. The electrochemical software was employed to analyze the experimental data (Version: 12.22.0.0). The experiments were carried out in a three-electrode glass cell equipped with a platinum auxiliary electrode and a saturated calomel reference electrode. 1 cm^2 of copper was used as the working electrode and it was implanted in polytetrafluoroethylene epoxy resin. The three electrodes immersed in 100 ml of control solution were allowed to reach open circuit potential (OCP) both in the absence and presence of inhibitors. By not tampering with the mixture, the pH of the solution was kept at 7 throughout the testing.

The polarization curves were acquired with a precision of 2 mV from −750 to −150 mV. Dynamic scan mode at 2 mVS^{-1} in the −20 to +20 mA range was used to record the curves. The Ohmic drop was accounted in the studies. The corrosion potential (E_{corr}), current (I_{corr}), anodic Tafel slope, and cathodic Tafel slope were all extrapolated from the anodic and cathodic Tafel plots respectively. IE_p value was determined from I_{corr} values, by using the following equation;

$$(\%)\mathbf{IE_p}\frac{\mathbf{I_{corr}}-\mathbf{I'_{corr}}}{\mathbf{I_{corr}}}\times 100$$

I_{corr} and I'_{corr} are blank, and corrosion-inhibited current densities.

At OCP, we measured the electrochemical impedance spectra at a frequency range of 60 kHz to 10 MHz, with a resolution of 4 to 10 steps per decade. Sine wave of 10 mV was used to jolt the system. A Nyquist plot was used to determine the resistance to charge transfer (R_{ct}) and double-layer capacitance (C_{dl}), and the following equation was used to get the protection efficiencies (IE_{im}).;

$$(\%)\mathbf{IE_{im}}\frac{\mathbf{R_{ct}}-\mathbf{R'_{ct}}}{\mathbf{R'_{ct}}}\times 100$$

Values for charge transfer resistance before (R_{ct}) and after the addition of an inhibitor (R'_{ct}) were provided.

2.3. Scanning electron microscopic (SEM)

The metal specimens were submerged in blank and the inhibitor solutions separetely. After seven days, the sample was collected, cleaned in triple-distilled water, allowed to air dry, and then examined under a scanning electron microscope for analysis. The VEGA3-TESCAN model was used to capture SEM images of the specimens' surfaces.

2.4. Energy dispersive analysis of x-ray (EDAX)

By connecting an EDAX (Model: BRUKER Nano Germany) to a scanning electron microscope, the elements on the copper covering were examined. This method examined a sample by exposing it to electromagnetic radiation. A detector was used to transform X-ray photons into electrical impulses. A pulse processor received these signals and analyzed them by a data display analyzer.

2.5. Atomic force microscope (AFM)

Surface roughness can be accurately measured with the use of AFM. As a result of these modern advancements, surface scanning can now be performed with greater precision and in detail. The protective film was scanned. More frequently, AFM is being used

to assess the roughness (Bharathi et al., 2012; Sukumar et al., 2012; Wang et al., 2022; Zahid et al., 2011). With the use of AFM, the variations in surface morphology (at a few hundred nanometers) brought on by the formation of corrosion and a protective layer containing and lacking inhibitors may be seen clearly. The Pico SPM2100 was used to take all of the AFM images in air contact mode. All of the AFM images were 15 by 15 μm and the scan rate were 0.20 Hz.

2.6. Water contact angle

By using sessile droplets, we empirically assessed the contact angle. A syringe provided life support for the sessile droplet. The substrate was photographed using a high-resolution camera (10.1 Mpixle SONY camera) while it was lit. A computer with the dedicated photo editing software was used to alter the image.

3. Results and discussion

3.1. Potentiodynamic polarization

Fig. 1 shows the potentio-dynamic polarization of copper in potable water at pH 7.84 with and without inhibitor. The Tafel parameters for corrosion of copper immersed in the potable water obtained by potentio-dynamic polarization studies with and without inhibitor are listed in Table 2. The corrosion potential and the corrosion current density of blank were found to be −0.038 mV/SCE and 6.837 A/cm^2 respectively as shown in Table 2. Tafel slopes at the anode and cathode were 67 and 119 mV, respectively. This could be attributed to the dissolution of copper at anodic sites leading to the formation of adsorbed Cu species (Cu^{+}_{ads}) and such anodic dissolution could be due to the following mechanism (Simonović et al., 2020).

$$Cu \leftrightarrow Cu_{ads}{}^{+} + e^{-} \text{ (fast)}$$

$$Cu_{ads}{}^{+} \leftrightarrow Cu_{sol}{}^{+} + e^{-} \text{ (slow)}$$

It was observed that for a solution containing 10 ppm Zn^{2+} and 100 ppm ST, the corrosion potential was shifted to −0.009 mV/SCE, and accordingly the corrosion current density also dropped when compared to the blank. The Tafel slope both at anode (81 mV) and cathode (136 mV) were found to be greater than that of blank. The reports conveyed if the hybrid inhibitors were present then the shift in the corrosion potential would be around or above 80 mV (Ferreira and Giacomelli, 2004; Li et al., 2008; Sudhakaran et al., 2015). From Table 2, it was noted that the current due to corrosion

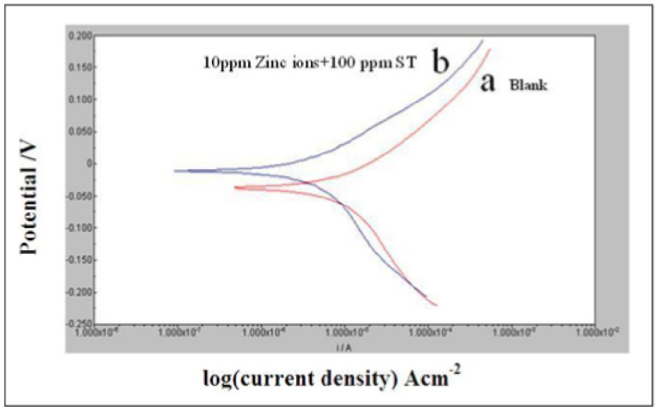

Fig. 1. Polarization curves for copper immersed in potable water in the absence (a) and presence (b) of sodium tartrate (Tafel plots).

was dropped from 6.837 A/cm^2 to 0.707 A/cm^2. The acquired data demonstrated that a protective layer was formed on the metal surface as a result of the presence of Zn^{2+} and ST inhibitors by reducing corrosion and metal disintegration, as demonstrated by the decrease in corrosion current density due to the presence of hybrid inhibitors. This was mainly due to the formation of complex between adsorbed copper species and inhibitor, viz. $[Cu^{+}\text{-Inh}]_{ads}$.

3.2. Electrochemical impedance spectroscopic studies

Nyquist plots for copper corrosion in potable water with and without inhibitors are displayed in Fig. 2. Table 3 provides the values for the charge transfer resistance (R_{ct}), double layer capacitance (C_{dl}), and inhibition efficiency (IE_{imp}). It was discovered that the rough electrode surface, which was reflected in the impedance diagram, was what caused the frequency dispersion (Zarrok et al., 2012). According to a report, the system's frequency affected the value of the charge transfer resistance (Sudhakaran et al., 2015). The frequency at which Zmax (ohms) is greatest can be used to compute the Cdl as given in the equation below;

$$\mathbf{f}(-\mathbf{Zmax}'') = \frac{1}{2\pi \mathbf{C_{dl}} \mathbf{R_{ct}}}$$

The equivalent electrical circuit depicted in Fig. 4 was used to fit the experimental data that was collected from Nyquist plots. A second constant circuit was employed simultaneously (Deepa et al., 2015; Appa Rao et al., 2010) to produce the same indented semicircles. Instead of using a simple double-layer capacitor, a constant phase element (CPE) was used here (Satapathy et al., 2009). From Table 3, the R_{ct} of the blank was found to be 107.09. From Fig. 3, a significant depressed semicircle in the Nyquist curves (b) was observed at low frequency direction and the diameter of semicircles was increased at high frequency direction in the presence of 10 ppm Zn^{2+} and 100 ppm ST, conveying that the charge transfer resistance became dominant in corrosion processes due to a protective coating on the copper surface.

The decreased C_{dl} and the increased R_{ct} values buttressed the results. The R_{ct} value of the semicircle was found to be 1317.43 when Zn^{2+} and ST were present. In addition to the lowering of i_{corr} and corrosion, a high R_{ct} value was also found to facilitate the mechanical stability (Zarrok et al., 2012). It was observed that the C_{dl} value at the metal/solution interface was found to decrease from 28.595 F/cm^2 (the blank case) to 0.185 F/cm^2 due to the presence of the binary inhibitor formulation. C_{dl} was found to be high because of the increased surface area of copper due to corrosion products (Sudhakaran et al., 2015). It was studied that the double layer thickness would have a negative effect on the capacitance (Deepa et al., 2015). Therefore, the decrease in capacitance was a sign of the inhibitor molecules adsorbing at the metal/solution interface, where the local dielectric constant would decrease, and the electrical double layer's thickness would increase. Therefore, it was proposed that a binary inhibitor strategy might enhance inhibition effectiveness by reducing interface inhomogeneity. The presence of the binary inhibitor would also result in a barrier. The report of this impedance study indicated that the inhibitory efficiency was found to be 92%. Hence, it was suggested that this would be also useful for potentio-dynamic polarization study.

3.3. SEM analysis

SEM was used to examine the surface morphology of copper while it was submerged in water and an inhibitor. Fig. 4a and 4b show the SEM images of copper surfaces with and without inhibitor. Corrosion, compromised metallic characteristics, and the surface corrosion products were all evident from Fig. 4 illustrating what would happen without the inhibitor formulation. Also, SEM

Table 2
Tafel parameters for corrosion of copper immersed in the potable water obtained by potentio-dynamic polarization studies both in the absence and presence of inhibitor.

Concentration (ppm)		Tafel parameters				IE_p (%)
ST	Zn^{2+}	E_{corr} mV vs SCE	i_{corr} A/cm^2 × 10^{-6}	β_a mV/decade	β_c mV/decade	
Blank	–	– 0.038	6.837	67	119	–
100	10	– 0.009	0.707	81	136	90

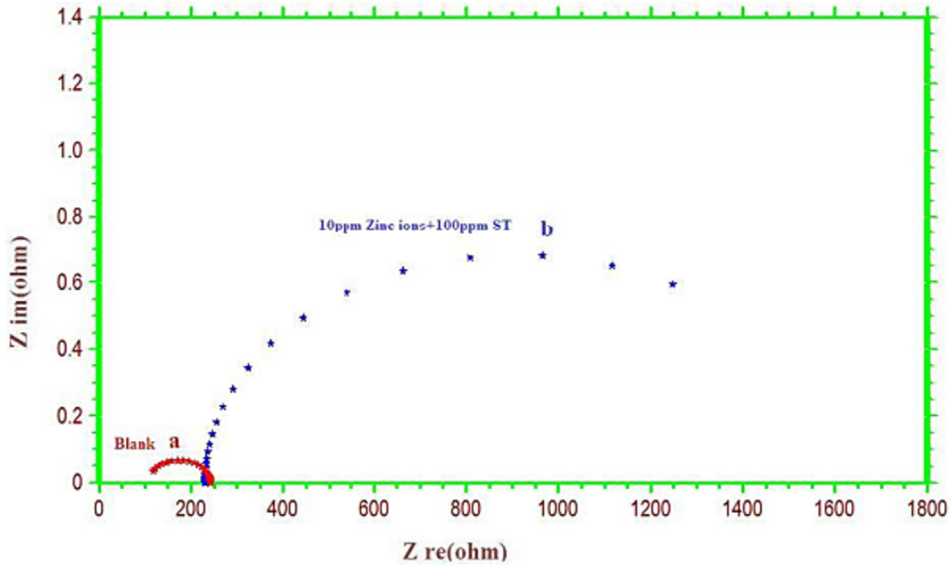

Fig. 2. Electrochemical impedance curves for copper in potable water (a) the absence and (b) presence of sodium tartrate (Nyquist plots).

Table 3
A.C impedance parameters for copper in potable water in the absence and presence of inhibitor obtained by A.C impedance spectra.

Concentration (ppm)		Charge transfer Resistance, R_{ct}(Ω)	Double layer capacitance, C_{dl} CPE µF/cm^2	IE_{imp} (%)
ST	Zn^{2+}			
Blank		107.09	28.595	–
100	10	1317.43	0.185	92

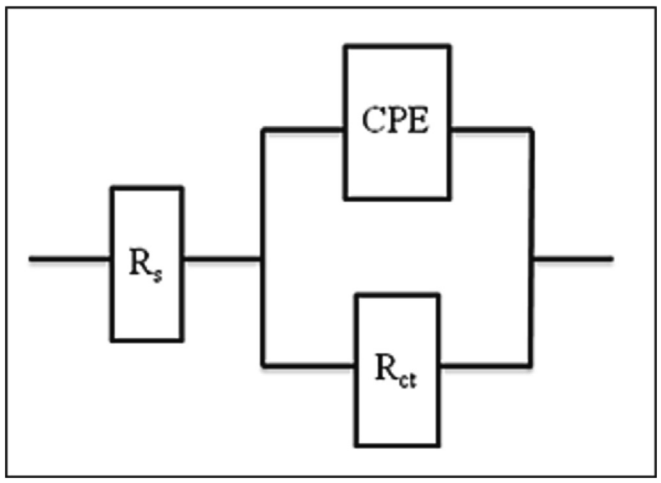

Fig. 3. Equivalent circuit employed to fit Nyquist plot.

image revealed a rough surface suggesting the uneven corrosion phenomenon in the absence of inhibitor as seen in Fig. 4b whereas smooth, polished surface of copper was observed in an inhibitor solution as seen in Fig. 4a.

The inhibitor had a significant impact on the structure of the copper surface. A uniformly dispersed protective coating was produced across the entire surface of the metal. The inhibitor's adsorption and subsequent absorption into the passive film inhibited the corrosion active site on the surface of copper, completely encasing the metal in the barrier. Thus, it was suggested that the high values of inhibitory efficiency found in the polarization investigations make sense. The inhibitor molecules covered the surface of copper and thus prevented further oxidation. Thus, the SEM study evidenced that the surface of the film could act as a protective layer (Sudhakaran et al., 2022).

3.4. EDAX analysis

The EDAX results of the copper coating analysis are displayed in Fig. 5. As shown in Fig. 5a, the damage due to corrosion of the cop-

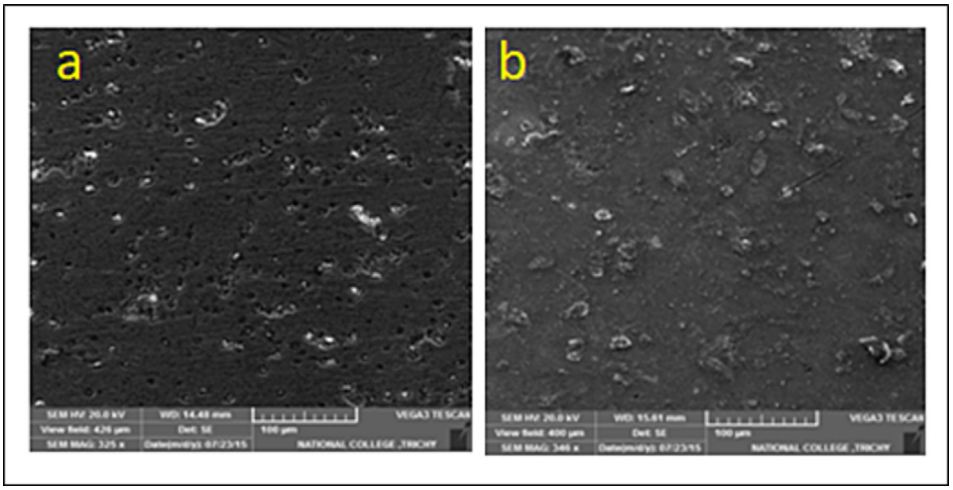

Fig. 4. SEM image of copper surface immersed in potable water (a) containing 10 ppm Zn^{2+} and 100 ppm ST, (b) without inhibitor.

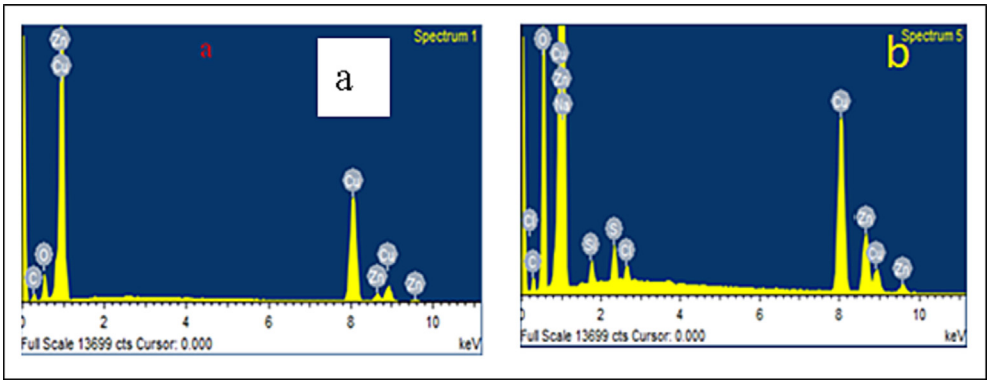

Fig. 5. EDAX analysis of copper surface (immersed in potable water) (a) without inhibitors; (b) with 10 ppm Zn^{2+} and 100 ppm ST.

per samples (CuO and Cu_2O) submerged in drinking water was observed without inhibitor molecules. Fig. 5b shows the EDAX spectrum of copper system with 10 ppm Zn^{2+}+100 ppm ST. As seen in Fig. 5b, the presence of a thick layer of inhibitor molecules on the sample's surface resulted in a weakening of the copper peak and the development of additional peaks attributable to carbon, oxygen, salt, and zinc [Amin, 2006]. As a result, it was proposed that inhibitors were adsorbed onto the electrode surface, whereupon they may create a protective layer. Thus, both SEM and EDAX analyses supported the formation of a copper barrier layer.

3.5. Atomic force microscopic (AFM) studies

In common, atomic force microscopy (AFM) focuses on the investigation of surface morphology by using a scanning probe with a very high resolution. The atomic force microscope (AFM) is a novel and advanced technique for analyzing the effect of inhibitors on corrosion at the metal/solution interface because of its ability to examine nano to microscale surface morphology [Satapathy et al., 2009]. From 2D and 3D images, we calculated the root-mean-square (R_{RMS}) roughness, the average roughness (R_a), and the maximum peak-to-valley height of the surfaces. AFM parameters for submerged copper surfaces are listed in Table S1 (*vide* supplementary file). The results showed that the immersion of copper in the blank without an inhibitor led to the formation of copper oxides as seen in Fig. 6a, which exhibited an increased R_a value of 64.5 nm, R_{RMS} of 88.6 nm, and maximum peak to valley height of 163.2 nm. The roughness of the corroded copper surface, measured as its root-mean-square R_{RMS}, was found to be 88.6 nm conveying the deposition of visible large and minute corrosion products on the surface microstructure of copper. Whereas both Ra and R_{RMS} were drastically decreased to 6.9 nm 7.4 nm respectively when copper was submerged in a solution containing 10 ppm Zn^{2+} and 100 ppm ST as shown in Fig. 6b due to the presence of more homogeneous surface when compared to that of blank without inhibitor.

With a peak-to-valley height of 23.4 nm and an R_{RMS} of 7.4 nm, it could be stated that the metal surface was coated for protection. The decrease in R_{RMS} value from 88.6 nm (in the blank) to 7.4 nm (in the presence of inhibitor) was the indication of increased coating uniformity and smoothness, as well as the absence of corrosion product deposition. The variance discovered in the optical cross-section study supported these findings. Thus, AFM analysis confirmed the formation of a coating on the surface of the metal to shield it from corrosion.

3.6. Water contact angle (WCA) measurement analysis

As illustrated in Fig. 7, the contact angle was used to determine the degree of wettability, or whether the substance was super hydrophobic or hydrophilic. From Fig. 7a, it was observed that the copper that was exposed to drinking water without an inhibi-

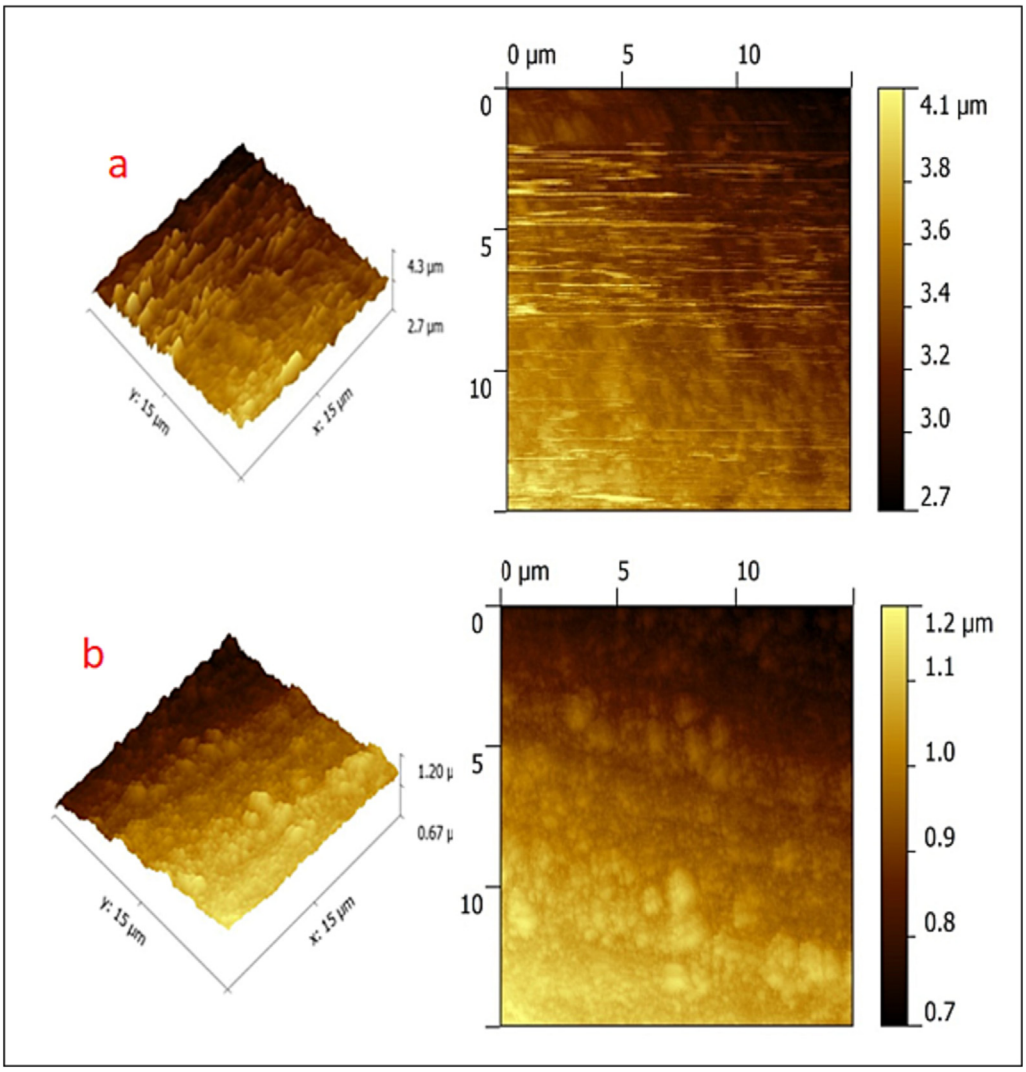

Fig. 6. AFM images of copper surface (immersed in potable water) (a) without inhibitors; (b) with 10 ppm Zn^{2+} and 100 ppm ST.

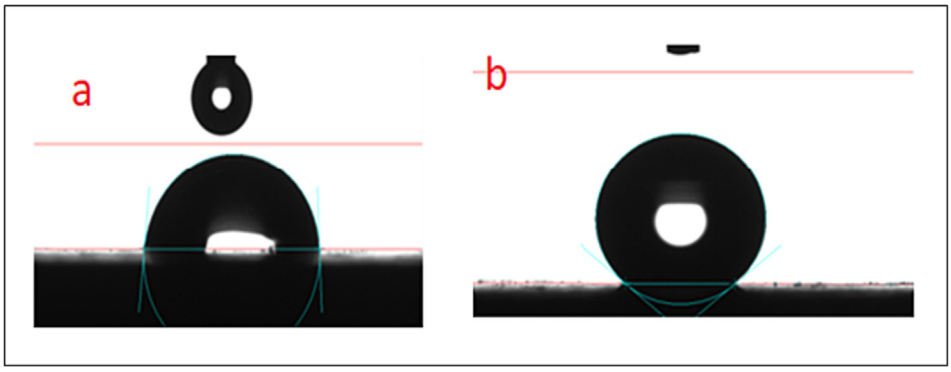

Fig. 7. WCA image of copper surface (immersed in potable water) (a) without inhibitors; (b) with 10 ppm Zn^{2+} and 100 ppm ST.

tor possessed a very porous and rough surface with a WCA of 83°2°. As shown in Fig. 7b, the WCA was seen to rise by 164°4° when the copper surface contained 10 ppm Zn^{2+} and 100 ppm ST, demonstrating that the surface became extremely hydrophobic. This was primarily caused by the coating of the inhibitor's polar group on the copper's surface whereas its non-polar group being directed towards the bulk solution, which produced a homogenous and hydrophobic contact. As a result, our work successfully established the existence of a copper surface with a superhydrophobic coating that is capable of adsorbing an inhibitor.

4. Conclusion

In this study, ST was reported as a potential corrosion inhibitor for copper in the potable water. Based on the polarization studies, it was confirmed that it was a hetero (mixed) type of inhibitor that could prevent the corrosion of copper. This study reported that the inhibitor including 10 ppm of Zn^{2+} and 100 ppm of ST attained a maximum corrosion inhibition efficacy of 92%. The findings of electrochemical impedance spectroscopy (EIS) demonstrated the formation of a protective coating on the surface of copper immersed in drinking water in the presence of inhibitor. The results obtained from SEM, EDAX and AFM images also confirmed the presence of a protective coating on the surface of the copper. Finally, the results of the contact angle tests, clearly conveyed that the coating formed on the surface of copper in the presence of inhibitor was indeed extremely homogeneous and hydrophobic in nature.

Declaration of Competing Interest

The authors declare that they have no known competing financial interests or personal relationships that could have appeared to influence the work reported in this paper.

Acknowledgement

The project was funded by Researchers Supporting Project number (RSP2023R231), King Saud University, Riyadh, Saudi Arabia

Appendix A. Supplementary material

Supplementary data to this article can be found online at https://doi.org/10.1016/j.jksus.2023.102921.

References

Amin, M.A., 2006. Weight loss, polarization, electrochemical impedance spectroscopy, SEM and EDX studies of the corrosion inhibition of copper in aerated NaCl solutions. J. Appl. Electrochem.. 36, 215–226.
Antonijević, M.M., Petrovic, M.B., 2008. Copper corrosion inhibitors. A review. Int. J. Electrochem. Sci. 3, 1–28.
Appa Rao, B.V., Venkateswara Rao, M., Srinivasa Rao, S., Sreedhar, B., 2010. Tungstate as a synergist to phosphonate-based formulation for corrosion control of carbon steel in nearly neutral aqueous environment. J. Chem. Sci. 122, 639–649.
Bharathi, P., Elavarasi, N., Mohanasundaram, S., 2012. Studies on rate of Biodegradation of Vegetable oil (Coconut oil) by using Pseudomonas sp. Int. J. Environment Biol. 2, 12–19.
Cabrin, M., Lorenzi, S., Coffetti, D., Coppola, L., Pastore, T., 2020. Inhibition effect of tartrate ions on the localized corrosion of steel in pore solution at different chloride concentrations. Buildings 10, 105.
Cao, C., 1996. On electrochemical techniques for interface inhibitor research. Corr. Sci. 38, 2073–2082.
Deepa, T., Thangavelu, C., Sekar, M., Sudhakaran, R., 2015. Corrosion inhibition of carbon steel in RO water using trisodium citrate - Zn2+ system. Asian J. Res. in Chem. 8, 613–617.
Feng, L., Yang, H., Wang, F., 2011. Experimental and theoretical studies for corrosion inhibition of carbon steel by imidazoline derivative in 5% NaCl saturated Ca (OH)2 solution. Electrochim. Acta. 58, 427–436.
Ferreira, E.S., Giacomellic, F.C., 2004. A. Spinelli, Evaluation of the inhibitor effect of l-ascorbic acid on the corrosion of mild steel. Mater. Chem. Phys. 83, 129–134.
Finšgar, M., Milošev, I., 2010. Inhibition of copper corrosion by 1,2,3-benzotriazole: A review. Corr Sci. 52, 2737–2749.
Habib, K., 1998. In-situ monitoring of pitting corrosion of copper alloys by holographic interferometry. Corr. Sci. 40, 1435–1440.
Kear, G., Barker, B.D., Walsh, F.C., 2004. Electrochemical corrosion of unalloyed copper in chloride media a critical review. Corr. Sci. 46, 109–135.
Khaled, K.F., Hackerman, N., 2003. Investigation of the inhibitive effect of ortho-substituted anilines on corrosion of iron in 1 M HCl solutions. Electrochim. Acta 48, 2715–2723.
Li, W.-H., He, Q., Zhang, S.-T., Pei, C.L., Hou, B.-R., 2008. Some new triazole derivatives as inhibitors for mild steel corrosion in acid medium. J. Appl. Electrochem. 38, 289–295.
Mohanasundaram, S., Ramirez-Asis, E., Quispe-Talla, A., Bhatt, M.V., Shabaz, M., 2022. Experimental replacement of hops by mango in beer: production and comparison of total phenolics, flavonoids, minerals, carbohydrates, proteins and toxic substances. Int. J. Syst. Assur. Eng. Manag. 13, 132–145.
Philip, A., Schweitzer, P.A., 2010. Fundamentals of Corrosion: Mechanisms, Causes, and Preventative Methods. CRC Press, pp. 1–4.
Ramesh, S., Rajeswari, S., 2005. Evaluation of inhibitors and biocide on the corrosion control of copper in neutral aqueous environment. Corr. Sci. 47, 151–169.
Satapathy, A.K., Gunasekaran, G., Sahoo, S.C., Amit, K., Rodrigues, P.V., 2009. Corrosion inhibition by Justicia gendarussa plant extract in hydrochloric acid solution. Corr. Sci. 51, 2848–2856.
Simonović, A.T., Tasćc, Z.Z., Radovanović, M.B., Mihajlović, M.B.P., Antonijević, M.M., 2020. Influence of 5–chlorobenzotriazole on inhibition of copper corrosion in acid rain solution. ACS Omega 5, 12832–12841.
Sudhakaran, R., Thangavelu, C., Sekar, M., Kasilingam, T., 2015. Electrochemical and surface studies of eco-friendly inhibitor in potable water system. Asian J. Res. Chem. 8, 16–20.
Sudhakaran, R., Deepa, T., Asokan, T., Govindaraj, M., Kasilingam, T., Babu, S., Sivarajan, A., 2022. Sodium gluconate as corrosion inhibitor for copper in potable water. Bull. Environ. Pharmacol. Life Sci. 1, 486–493.
Sukumar, M., Jayaseelan, A., Sivasankaran, T., Mohanraj, P., Mani, P., Sudhakar, G., Arumugam, V., Bakthavachalu, S., Ganesan, A., Susee, M., 2012. Production and partial characterization of Extracellular Glucose Isomerase using Thermophilic Bacillus sp. isolated from agricultural land. Biocat. Agri. Biotech. 2, 45–49.
Szőcs, E., Vastag, G., Shaban, A., Kálmán, E., 2005. Electrochemical behaviour of an inhibitor film formed on copper surface. Corr. Sci. 47, 893–908.
Wang, Q., Sivakumar, K., Mohanasundaram, S., 2022. Impacts of extrusion processing on food nutritional components. Int. J. Syst. Assur. Eng. Manag. 13, 364–374.
Zahid, I., Gopinath, K., Sivakumar, M., Mohanasundaram, P., Ramesh, R., 2011. Studies on removal of Malachite green from the aqueous solution by sorption method using water Hyacinth-Eichornia crassipes roots. J. Biodiver Environ. Sci. 2, 1–8.
Zarrok, H., Oudda, H., Midaoui, E.I., Zarrouk, A., Hammouti, B., Ebn Touhami, M., Attayibat, A., Radi, S., Touzanu, R., 2012. Some new bipyrazole derivatives as corrosion inhibitors for C38 steel in acidic medium. Res. Chem. Intermediates. 38, 2051–2063.